IEEE Access
Multidisciplinary ⋮ Rapid Review ⋮ Open Access Journal

Received May 18, 2020, accepted May 31, 2020, date of publication June 9, 2020, date of current version June 22, 2020.

Digital Object Identifier 10.1109/ACCESS.2020.3001189

Graphical Topology Autonomic Identification Method for Human-Machine Interface Modelling Based on Quadratic Space Mapping

YANJUAN WU[1], HAOYUE WANG[1], YUNLIANG WANG[1], AND LI YANG[2]
[1]Tianjin Key Laboratory for Control Theory and Applications in Complicated Systems, Tianjin University of Technology, Tianjin 300384, China
[2]State Grid Chongqing Electric Power Company Yongchuan Power Supply Branch, Chongqing 402160, China

Corresponding author: Yanjuan Wu (wuyanjuan12@126.com)

This work was supported by the State Grid Chongqing Electric Power Company Science and Technology Project Funding [Grant number SGTYHT/17-JS-199], the Tianjin Science and Technology Plan Project [Grant number 18ZXYENC00100] and the National Natural Science Foundation [Grant number 51877152].

ABSTRACT To realize a computerized autonomous recognition of human-computer interface graphics and autonomously interface an interface graphic model with a simulation analysis program of a systems operation, a human-computer interface topology identification algorithm based on quadratic space mapping (QSM) is proposed, which includes three mapping spaces and two mapping methods. The three mapping spaces are defined as the interface modelling graphics space, the primitive information space and the abstract topology space. The first mapping method uses hierarchical topology mapping based on coordinate properties, and the second uses abstract topology mapping based on breadth first search. The QSM algorithm converts a visual graphical physical model on a human-machine interface into a computer-recognizable abstract model. Then, a simulation analysis of the system is performed automatically by a computer using the converted abstract model. Finally, taking the distribution network system as an example, the proposed topology recognition algorithm realizes the conversion of the interface modelling graph to the abstract model of the distribution network. Furthermore, the simulation of the power flow algorithm is performed by interfacing perfectly with the abstract model, and the feasibility and practicability of the algorithm are verified.

INDEX TERMS Computerized autonomic identification, human-machine interface graphical modelling, quadratic space mapping, graphical topology recognition, abstract topology.

I. INTRODUCTION

With the continued development of science and technology, many complex systems have higher requirements for safe and reliable operation, especially for expensive systems such as power grids, aerospace applications, military equipment, and so on. Once operational failures occur, they can cause considerable economic losses. It is generally not permissible or practical to perform operational tests directly on these actual systems. Before computer-aided analysis technology was developed, to ensure the safe operation of these complex systems, it was only possible to divide a system into several small systems and conduct local tests, which resulted in the inefficient use of time, finances and material resources. With the development of computer-aided analysis technology, these complex systems can be assessed by computerized simulation-aided analysis, which saves considerable manpower, material and financial resources and indirectly promotes the development of these systems to a more complex and larger scale, such as power systems, communication systems and so on. The application of computer-aided analysis technology has also been continuously expanded to industry, agriculture, medical health, economic analysis, social services, and the currently rapidly developing robotics field [1]–[6].

The topological analysis method is one of the most commonly used computer-aided analysis methods for identifying the connection relationships of complex systems. The topology analysis methods of system modelling can be divided into static topology analysis and dynamic topology analysis.

The associate editor coordinating the review of this manuscript and approving it for publication was Ruisheng Diao.

Computerized static topology analysis is an off-line analysis method that has a high accuracy for the steady-state analysis of a system, but errors can occur in the dynamic analysis of the system. Using computer-aided dynamic topology analysis is more accurate for analysing the dynamic changes of complex systems in real time. Literature [7] identified a distribution network topology based on system operation measurement data; literature [8] obtained a topology structure based on system monitoring parameters; literature [9] identified nontree topologies based on system data for single-source networks; literature [10] realized smart grid topology identification based on graph theory combined with sparse recovery technology; literature [11] restored the topology of an entire feeder in a power grid based on the detected voltage value by installing detectors on all nodes, and literature [12] obtained the topology of a distribution network through the probability relationship between different voltage measurements. The above studies were used to obtain the real-time topology relationship of a constructed actual system. The topological relationships were obtained from already constructed systems in real time, and then system simulation operation and optimization were performed according to the topology relationship. However, these methods of real-time online simulation analyses are not combined with visualization. The topological structure of a system is obtained by analysing the measured data using probabilistic methods that will lead to some degree of deviation between the topology model and the actual system, and it is difficult to expand the scale of the system more conveniently and intuitively due to the lack of visualization. With the development of computer object-oriented graphics technology, many systems have begun to use computers for graphical visualization modelling and simulation analysis. This approach realizes that the components of the system are drawn on the human-machine interface to form a visual system model based on the topological relationship of the actual system; thus, it can use the computing power of the computer to simulate the operation of the system, which can not only realize the visualization of the system topology but can also more accurately and more quickly analyse the system operation. If the visualization and system operation data are combined to obtain the topology model in real time, it will be more accurate and closer to the actual system.

Visual computer-aided analysis combined with a visual system model on a human-machine interface can more intuitively reflect the dynamic changes of a system and allow engineers to obtain the topological structure more quickly and accurately. Literature [13] proposed a visual analysis method of inertial particle force-induced dynamics by an integrated topological analysis method. Literature [14] proposed a topology visual analysis method of community complex networks, which can analyse community dynamics and fusion problems in real time. Literature [15] used the topological extraction method to identify images and visualize the recognition process. These studies on system topology identification can address the needs of complex system topology modelling and achieve system visualization but have not realized an interface with system simulation algorithms. To analyse and study the operation of these system more accurately, it is necessary not only to construct a visual system model consistent with the actual system but also to automatically interface with a system simulation running program. However, to realize a system visual simulation operation analysis, the following key technologies need to be involved:

1. It is necessary to establish a human-machine interface visualization system model (HMIVSM) that can accurately reflect the connection relationship of various components in an actual system (CRCS). This key technology establishes an HMIVSM by using easy-to-understand and consensus-driven graphics, which enables operators to more clearly understand the structure and composition of the system and the interconnection of the system components.
2. Information processing techniques are needed to address the operational characteristics of the actual system (OCS) and the physical characteristics of each component of the actual system (PCCS). The established HMIVSM only represents the CRCS but does not express the OCS and the PCCS. Therefore, it is necessary to study the information processing technology that interfaces the OCS and the PCCS with the HMIVSM and that can be autonomously recognized by the computer.
3. An abstract topology transformation technique needs to be established. Using abstract topology, information that includes the topological connection information of the HMIVSM, the OCS and the PCCS can be directly called by the programs of the system operation simulation analysis algorithm (PSOSAA).

Though the above key technologies, the HMIVSM is established, the OCS and the PCCS are interfaced to the HMIVSM, and then CRCS, OCS and PCCS information is interfaced to the PSOSAA. Through the close cooperation of these three key technologies, the simulation operation analysis of the HMIVSM can be truly completed. At present, most of the existing research has focused on the combination of key technology 1 and key technology 2 or the combination of key technology 2 and key technology 3. The former, as seen in previous literature [13]∼[15], studied computer visualization but did not realize the interface with the system simulation algorithm. There are also many studies on the latter: literature [16] studied a real-time simulation platform of a 400 V-50 KVA digital physics hybrid power system; literature [17] studied a real-time simulation technology for power system design, testing and analysis; literature [18] proposed an integrated modelling and simulation analysis of engineering complex systems; and literature [19] applied the DecompositionJ framework and co-simulation platform to power grid research. These studies only examined system simulation models and did not realize system visualization. Most topology studies only identify the topology of graphs but do not directly interface the graph topology with the PSOSAA. When the topology graphics change, a professional is required to modify the programs of the simulation

algorithm, which will lead to certain application limitations. That is, in many current research methods, system graphics visualization and system simulation analysis are actually separated, and even the HMIVSM is only used as a display function. The CRCS, OCS and PCCS cannot be identified by the computer autonomously. Few studies provide a complete and effective solution that can simultaneously complete the construction of an HMIVSM, a computerized autonomous identification of an HMIVSM and a system operation simulation analysis synchronized with an HMIVSM. Therefore, it is necessary to study a conversion method of an abstract topology model, which can realize computerized automatic identification of an HMIVSM and complete the interface of an HMIVSM with the programs of a system operation simulation algorithm.

The application of space mapping theory has advantages in topology analysis and problem optimization: for example, a self-organizing mapping method of a topological clustering polar was proposed for the cluster analysis of unmarked data sets [20]; a self-organizing mapping method of topological data was proposed for hierarchical clustering analysis [21]; a mapping matrix and NSGA-II achieved multiobjective topology optimization of the Internet of Things [22]; a mapping algorithm was used to analyse virtual networks [23]; a topology mapping algorithm was applied to an intelligent cloud test platform [24]; a topological mapping method was researched for a multiscale fusion network simulation [25]; and spatial mapping was used to optimize energy conversion in electromagnetic equipment [26].

In terms of the previous research, the computerized automatic identification of an HMIVSM is very complex, and it is difficult to realize by direct mapping. This paper proposes an algorithm that uses quadratic space mapping (QSM) to realize the computerized automatic identification of an HMIVSM. The mapping spaces are defined, the mapping methods are given, and the HMIVSM is converted into an abstract model that can be automatically identified by the computer. The proposed algorithm realizes that the visualization graphics topology of the system is automatically identified by the computer and then directly interfaces with the programs of the system operation simulation algorithm.

The preliminary work of this paper researches the method of establishing an HMIVSM based on Microsoft Foundation Classes (MFC) primary development [27]. The highlights of this work are as follows:

1. A method based on the human-machine interface graphic coordinates and the establishment of multidimensional arrays is proposed to realize the autonomous identification of an HMIVSM. Using this method can ensure that the connection relationship between the components of the HMIVSM is consistent with that of an actual system, and the information of the OCS and the PCCS is consistent with that of the actual system, which ensures modelling and recognition accuracy.
2. A QSM method is proposed. This method uses the secondary transformation method of multidimensional array space, in which the first transformation realizes the interface of the information between the actual system and the HMIVSM, and the second transformation completes the interface of the information between the HMIVSM and the PSOSAA: the information includes the CRCS, the OCS, and the PCCS.
3. An abstract topology method based on the breadth first search is proposed. By this method, the computer can autonomously identify the data information of the HMIVSM and construct an abstract topology that can be directly identified and used by the computer system operation analysis program. That is, the method can allow the computer to directly interface the HMIVSM with the PSOSAA.

This paper is organized as follows: Section II provides an overview of the theory and application of QSM. Section III proposes the QSM method and describes its specific implementation method. Section IV verifies the effectiveness of the QSM method by taking a distribution network system as an experimental example. Finally, the conclusions and further research are described.

II. TOPOLOGY RECOGNITION BASED ON QSM

A. QSM

Mapping enables the conversion from one space to another space or from a real space to an abstract space. The mapping method must truly reflect the characteristics of the model being transformed. QSM can provide a theoretical method for the computerized autonomic identification of an HMIVSM and for the interface of information that includes the CRCS, the OCS, and the PCCS between the HMIVSM and the PSOSAA.

For a complex system such as a power system, it is difficult to directly transform the interface visualization topology space to the computer calculation space of a system operation simulation algorithm. The QSM refers to the process in which the complex problem is simplified by quadratic spatial conversion [28]. Therefore, the application of QSM can play a role in buffering and simplification. Its mathematical expression is shown in equation (1).

$$\begin{aligned} C_1 &\xrightarrow{g} C_2 \xrightarrow{f} C_3 \\ F_1(C_1) &= F_2(C_2) = F_3(C_3) \end{aligned} \tag{1}$$

where $C_i (i = 1, 2, 3)$ is the performance form of the problem in the i-th space, $F_i (i = 1, 2, 3)$ is the description function, and g and f are mapping functions.

The three topology spaces are defined as the interface modelling graphics space (IMGS), the primitive information space (PIS) and the abstract topology space (ATS). The mapping process is shown in Fig. 1.

The three spaces in Fig. 1 correspond sequentially to C_1, $C_2$and C_3 in formula (1), and mapping mode 1 and mapping mode 2 in Fig. 1 correspond to g and f respectively in formula (1).

FIGURE 1. Schematic diagram of the mapping process.

B. SPACE DEFINITION

1) IMGS

The interface modelling graphics space is an interface working area formed by the pixels of the computer human-machine interface. A global coordinate is set in the interface working area, and it can be assumed that the point at the top left of the interface area is the starting point (0,0) of the coordinate. The HMIVSM can be drawn in this interface working area which shows the user an intuitive system. The computer human-machine interface is only used to display the graphical model of the actual system, but the topology relationship and physical properties of the system cannot be identified automatically by the computer itself.

2) PIS

The primitive information space is an intermediate transition space, which is layered according to the property of the primitive. The same property of different primitives in the HMIVSM is defined as a layer. There are a total of four layers. The first layer is the coordinate property layer, the second layer is the base property layer, the third layer is the base property layer of the out-connection primitives, and the fourth layer is the physical property layer. A hierarchical structure schematic of the PIS is shown in Fig. 2.

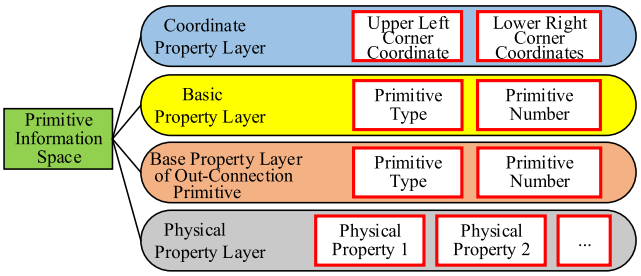

FIGURE 2. Schematic of primitive information space.

The front three layers reflect the position of the primitive itself and its topology connection relationship with other primitives. Therefore, the content of the front three layers is stored in the primitive topology information array (PTIA). The content of the fourth layer is individually stored in the primitive physical information array (PPIA). Through the intermediate transition space, the types, functions, physical properties and structural connection relationship of different primitives can be sorted in an orderly manner, which provides favourable conditions for the subsequent more accurate and quicker conversion of the PIS to the ATS using mapping mode 2.

3) ATS

The abstract topology space includes the topology point information array (TPIA) and the topology line information array (TLIA). The TPIA includes physical information of all points extracted from the PPIA in the PIS. The TLIA includes the physical information and the connection relationships of all lines extracted from the PPIA in the PIS. Thus, an abstract topology is built that can be interfaced directly with the PSOSAA. The point of the abstract topology contains the physical property information of each primitive in the IMGS, and the line of the abstract topology represents the actual connection relationship of each primitive in the IMGS.

Through mapping mode 1, the information about the location, physical properties and topology connection relationship of the primitive in the IMGS is collected and stored into two arrays in the PIS. Then through mapping mode 2, the information of two arrays in the PIS is extracted and normalized into an abstract topology form that can be directly called by the PSOSAA. In this way, the computer can automatically realize the interface of the HMIVSM with the PSOSAA. The QSM method enables the computer to automatically recognize the HMIVSM and then automatically perform an operation simulation analysis of the identified system. The specific implementation method is described as follows.

C. THE MAPPING METHOD AND MAPPING PROCESS

According to the mathematical model of the QSM in formula (1), the conversion relationship among the IMGS, the PIS and the ATS can be expressed in mathematical expression as shown at the bottom of this page, where $C_{\text{Interface modeling (Graphics)}}$, $C_{\text{Primitive information (Property array)}}$ and $C_{\text{Abstract topology (Point line relationship array)}}$ represent the topologies in the IMGS, PIS and ATS, respectively.

F_i (i = 1,2,3) is the description function of the topology in the corresponding space.

g is the mapping function from the IMGS to the PIS, which corresponds to mapping mode 1 in Fig. 1, so mapping mode 1 is also called g mapping. f is the mapping function from the PIS to the ATS, corresponding to mapping mode 2 in Fig. 1, so mapping mode 2 is also called f mapping.

1) MAPPING MODE 1

The topology in the HMIVSM is the physical topology graph drawn by the user according to the actual system. The role

$$C_{\text{Interface modeling(Graphics)}} \xrightarrow{g} C_{\text{Primitive information (Property array)}} \xrightarrow{f} C_{\text{Abstract topology(Point-line relationship array)}}$$
$$F_1\left(C_{\text{Interface modeling (Graphics)}}\right) = F_2\left(C_{\text{Primitive information(Property array)}}\right) = F_3\left(C_{\text{Abstract topology (Point-line relationship array)}}\right)$$

of g mapping is to extract the property information of each primitive in the HMIVSM and convert them into the PIS. The primitive identification and transformation rules of the g mapping include the following four parts.

(1) Coordinate property mapping of the primitives. The coordinate identification method is used to realize computerized autonomous recognition of the connection relationship for the primitive in the HMIVSM. The top left corner of the interface is defined as the starting point (0,0) of the global coordinates, and the upper left coordinate information and the lower right coordinate information of each primitive can be obtained by the global coordinates. Therefore, the location information and region range information of the primitives in the HMIVSM can be mapped to the PIS.

(2) Base property mapping of the primitives. According to the function in the actual system operation, the primitives in the HMIVSM are divided into different function types that can be automatically marked when they are drawn or input. The base property mapping of primitives achieves primitive type identification and serial number identifiers of the same type of primitives and then converts this information to the PIS.

(3) Base property mapping of the out-connection primitives. The HMIVSM is a visual model that reflects the connection relationship of various components in the actual system. A graph representing a component is called a primitive. There must be interconnections between the primitives. To realize an automatic interface of the HMIVSM with the PSOSAA, it is necessary to identify this kind of connection relationship. To prevent confusion, reduce memory usage, and increase conversion speed, only out-connection primitives are recorded. Therefore, it is also necessary to record the function type and the sequence number of the out-connected primitives.

(4) Physical property mapping of the primitives. Each primitive of the HMIVSM has a corresponding physical meaning in the actual system, and its physical parameters can be input by a mouse or by a specified file in advance. Then, the physical parameters are automatically searched by the computer based on its coordinate properties.

2) MAPPING MODE 2

Mapping mode 1 maps the property information of each primitive to the PIS, but the orderly interconnection between the primitives is not fully reflected. That is, it only completes the collection of the primitive information, but this information is disorderly and cannot be directly identified and used by the PSOSAA. Therefore, f mapping is needed to classify the scattered primitive information of the PIS and then convert it into overall ordered topology information. The rules of the f mapping are described as follows.

(1) Point-line relationship mapping of the system. According to the specific requirements of the specific system analysis, the points and lines are classified from the primitives to form a point-line relationship topology [29], [30], and the topology identification can be performed by this kind of the point-line relationship. In general, the equipment, devices and connected components in the system are taken out as points, and the physical or logical connections between the various points are taken out as lines. In this way, the abstract topological relationship of the entire system is obtained.

(2) Network topology mapping. The methods commonly used in network topology recognition are mainly tree search methods, including breadth first search (BFS) and depth first search (DFS). Both tree search methods perform network topology analysis by searching for neighbour points of the target point [29]. DFS search will repeatedly search for some points, so it has to backtrack the previous point repeatedly, which makes the overall search speed slower than BFS, and its search process takes up more memory.

The steps of the BFS search method are shown as follows.

(a) A starting point is arbitrarily selected as a target point from the topology of the PIS.

(b) All points adjacent to the target point are searched from the PIS and stored in the adjacent point set in turn.

(c) The points in the adjacent point set obtained by searching in (b) are taken out in turn which is denoted as A_i; the target point is updated to A_i simultaneously, and the loop step (b) is updated until all points are searched completely.

Take the point-line diagram extracted from the topology of the PIS shown in Fig. 3 as an example. The starting point is taken as A_0. The search sequence of the BFS is as follows: $A_0 \rightarrow A_1 \rightarrow A_2 \rightarrow A_3 \rightarrow A_8 \rightarrow A_4 \rightarrow A_{10} \rightarrow A_9 \rightarrow A_5 \rightarrow A_6 \rightarrow A_{11} \rightarrow A_7$.

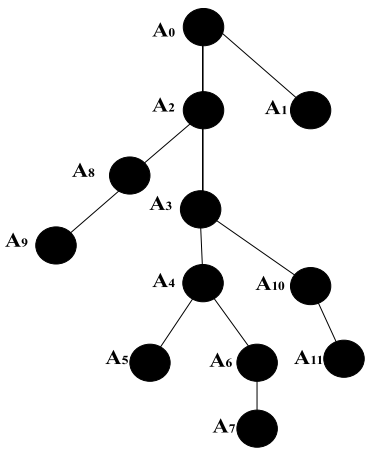

FIGURE 3. Point-line topology diagram.

3) MAPPING PROCESS

The target of space mapping allows the computer to automatically interface the HMIVSM with the PSOSAA.

The IMGS is a two-dimensional planar space, the PIS is a high-dimensional array space containing four layers property of the primitives, and the ATS contains two arrays—the

TPIA and the TLIA. Each primitive drawn in the HMIVSM has a corresponding coordinate range, and various property information of the primitive can be determined through the coordinate property. Therefore, mapping mode 1 is a hierarchical topology mapping based on coordinate properties. Although mapping mode 1 is a complex topology process, it can finally solve and simplify topology recognition and help the computer fully understand the topological relationship of the primitives in the HMIVSM.

Mapping mode 2 is an abstract topology mapping based on BFS. This is a topology simplification process in which the high-dimensional array in the PIS is converted into two two-dimensional arrays which can be called directly by the PSOSAA.

Through the QSM mentioned above, the HMIVSM can be converted into an abstract topology recognized autonomously by the computer. Using the abstract topology, the computer can implement an operation simulation analysis of the HMIVSM with analysis algorithms.

III. AUTONOMIC IDENTIFICATION METHOD FOR THE HMIVSM

To realize the autonomic recognition of the HMIVSM, the first step is to map the IMGS to the PIS. The computer needs to identify each primitive by the coordinate property. It identifies not only the function type of each primitive but also the connection relationship between the primitives [31].

To realize the coordinate recognition and the connection relationship identification of the primitives in the HMIVSM, a bounding box is set for each primitive. The bounding box is the smallest rectangle that can frame the primitive [32]. A schematic of the bounding box is shown in Fig. 4.

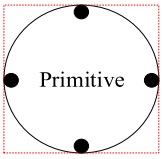

FIGURE 4. Primitive setting bounding box.

The red dashed line in Fig. 4 is the boundary box for placing the primitive. After the boundary box is set, the type identification function of the primitive can be performed. To further identify the interconnected relationship between the primitives, it is necessary to set the connection identification point of the primitive on the boundary box in Fig. 4. The black dots at the midpoints of the four sides are set as connection identification points. One primitive usually has in-connection points and out-connection points, and their number may be one or more. The out-connection point of the primitive is set as the property of the primitive connection identification point in this paper.

After the boundary box of the primitive is set, the topology relationship identification of the primitives in the HMIVSM is realized by computer programming. The flow chart of the programming is shown in Fig. 5.

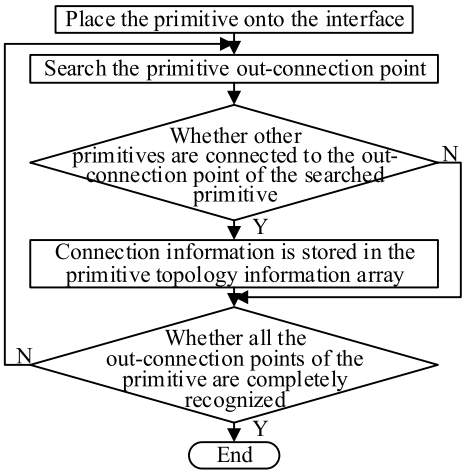

FIGURE 5. The program flow chart for real-time searching of the topology relationship of the primitives.

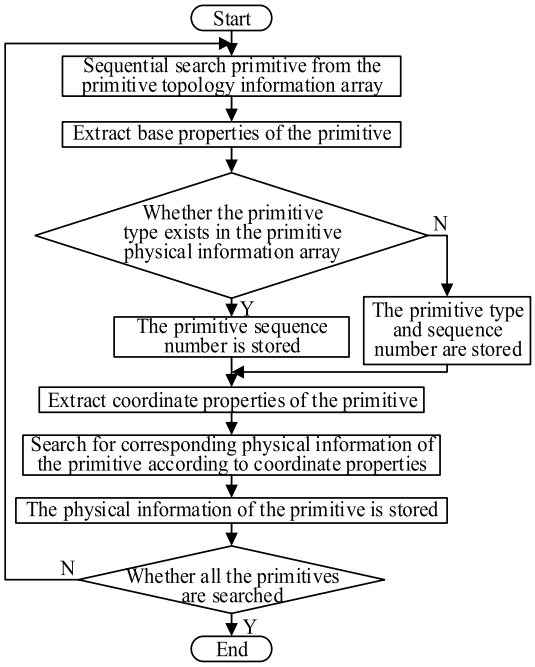

FIGURE 6. The PPIA program flow chart.

The program flow chart of the primitive physical information array is shown in Fig. 6.

The properties of the front three layers in Fig. 2 are stored in the PTIA, and the fourth layer property is stored in the PPIA. The relationship between the two arrays is built by the second layer property. By mapping model 1, the two-dimensional array space of the HMIVSM is converted into the high-dimensional dynamic array space of the PIS.

1) PTIA

The PTIA is a three-dimensional array. It is shown in formula (2).

$$\boldsymbol{A} = \begin{Bmatrix} \boldsymbol{A}_1 & \boldsymbol{A}_2 & \boldsymbol{A}_3 \end{Bmatrix} \tag{2}$$

where $\boldsymbol{A}_1$, $\boldsymbol{A}_2$ and $\boldsymbol{A}_3$ are the first dimension, the second dimension and the third dimension, respectively.

The first dimension array is shown in formula (3):

$$\boldsymbol{A}_1 = \begin{pmatrix} a_1 & a_2 & \cdots & a_i & \cdots \end{pmatrix} \tag{3}$$

where a_i is the sequence number of the i-th primitive in the HMIVSM, and the dimension of the first dimension can be set to an appropriate value according to the scale of the system.

The i-th row vector in the second dimensional array is shown in formula (4):

$$\boldsymbol{A}_{2a_i} = \begin{pmatrix} a_{i1} & a_{i2} & \cdots & a_{ik} \end{pmatrix}_{a_i} \tag{4}$$

where $\boldsymbol{A}_{2\boldsymbol{a}_i}$ is the i-th row vector including k property elements in the second dimensional array, and a_{ik} is the k-th property identifier of the i-th primitive a_i.

The dimension of the second dimension is $k \geq 3+n$, where 3 represents the three properties of the i-th primitive a_i itself that include the coordinates of the upper left corner of the i-th primitive, the coordinates of the lower right corner of the i-th primitive, and the base property of the i-th primitive. n represents the number of out-connection points of the i-th primitive. Considering that number of out-connection points may be different for different primitives, n takes the maximum value of all the numbers.

The coordinate information of the PTIA will be updated and modified in real time when the position of the primitive moves or be deleted in the working area of the interface; moreover, it must ensure that other relevant information is also updated and modified synchronously. Using the coordinate information of the primitives, their physical information can be searched, and the PPIA is completed by mapping mode 1. When the physical property parameters of the primitive are changed and corrected, the location stored in PPIA is also found through the coordinate information of the primitive, and the real-time modification is executed correspondingly. Therefore, the PIS is also a high-dimensional dynamic array space.

The base property of the PTIA is used to identify the functional property of the primitive. It is used to complete the point and line classification of the primitive in the conversion process of mapping mode 2.

The base property of the primitive out-connection in the PTIA is used to obtain the interconnection relationship between the primitives. It is conducive to the formation of abstract topological connections in the process of abstract topological space mapping (mapping mode 2).

The third dimensional vector$\boldsymbol{A}_{3a_{ik}}$defines the two properties of a_{ik}, which are the elements of the i-th row and the k-th column in the second dimensional array, and it is shown as follows:

$$\boldsymbol{A}_{3a_{ik}} = \begin{pmatrix} b_{k1} & b_{k2} \end{pmatrix}_{a_{ik}} \tag{5}$$

where $\boldsymbol{A}_{3\boldsymbol{a}_{ik}}$is also called the k-th property vector of the i-th primitive.

b_{k1}andb_{k2}record the real-time values of the k-th property corresponding to the i-th primitive.

The coordinate property is two-dimensional, which includes the abscissa and the ordinate. The base property of the primitive is two-dimensional, which includes the function type identifier and sequence number of the primitive. The base property of the out-connected primitive is also two-dimensional, which includes a function type identifier and sequence number; therefore, the dimension of the third dimension is 2.

2) PPIA

The PPIA is a three-dimensional array which is shown in formula (6).

$$\boldsymbol{P} = \begin{Bmatrix} \boldsymbol{P}_1 & \boldsymbol{P}_2 & \boldsymbol{P}_3 \end{Bmatrix} \tag{6}$$

where $\boldsymbol{P}_1$, $\boldsymbol{P}_2$and $\boldsymbol{P}_3$ are the first dimension, the second dimension and the third dimension, respectively.

The first dimension array is shown in formula (7):

$$\boldsymbol{P}_1 = \begin{pmatrix} p_1 & p_2 & \cdots p_s & \cdots \end{pmatrix} \tag{7}$$

where p_s is the s-th function type of the primitive, and the dimension of the first dimension is the total number of primitive function categories.

The s-th row vector in the second dimensional array is shown in formula (8):

$$\boldsymbol{P}_{2p_s} = \begin{pmatrix} p_{s1} & p_{s2} \cdots & p_{st} & \cdots \end{pmatrix}_{p_s} \tag{8}$$

where $\boldsymbol{P}_{2p_s}$ is the s-th row vector including the sequence number of all primitives belonging to the s-th function type. p_{st} is the sequence number of the t-th primitive in the s-th function type. The dimension of the second dimension can be set to an appropriate value according to the scale of the system.

The third dimensional vector $\boldsymbol{P}_{3\,P_{st}}$ defines the physical property of p_{st}, which is the element of the s-th row and the t-th column in the second dimensional array, and it is shown as follows:

$$\boldsymbol{P}_{3p_{st}} = \begin{pmatrix} q_{t1} & q_{t2} & \cdots & q_{tu} & \cdots \end{pmatrix}_{p_{st}} \tag{9}$$

where $\boldsymbol{P}_{3p_{st}}$ is also called the physical property vector of the t-th primitive in the s-th function type. q_{tu} records the values of the u-th physical property of the t-th primitive in the s-th function type, and the third dimension is set according to the maximum number of physical properties among all the primitives.

After the primitive boundary box and the connection identification point are completed by the programming, the computer can automatically recognize the primitives placed in the HMIVSM and then store the topology connection relationships and physical information of each primitive into the two arrays mentioned above. In this way, the mapping from the IMGS to the PIS is completed, and it is also prepared to finally realize the abstract topology that can be identified by a computer.

A. IMPLEMENTATION METHOD OF MAPPING MODE 2

After the computerized autonomous identification of the HMIVSM is completed by mapping mode 1, the interface primitive connection relationship and the physical property value are stored into the PTIA and the PPIA, respectively, in real time. By mapping model 1, the classification identification of the primitives in the HMIVSM is also completed. However, the classification is disordered and cannot be called directly by the PSOSAA. Therefore, mapping mode 2 is needed to convert the PIS into the ATS. It can realize the ordering and sorting of the primitive information. The ordered abstract topology can be autonomically identified by a computer and interfaced perfectly with the PSOSAA.

Mapping method 2 uses the BFS search method to obtain the abstract topology. The abstract topology includes two arrays—the TPIA and the TLIA.

(1) The TPIA is a two-dimensional array. The first dimension is the serial number, and the storage content in the second dimension includes the point search serial number, point information number and physical information of the point in the system.
(2) The TLIA is a two-dimensional array. The first dimension is the serial number, and the storage content in the second dimension includes the line search serial number, the search sequence number of the first point in the connection line, the search sequence number of the end point in the connection line, and the physical information of the connection line in the system.

The steps for the abstract topology implementation are described as follows.

(a) Only the primitives with out-connection properties (or the system model specified primitives) form a critical point set, and the first primitive is taken as the target primitive in the critical point set.
(b) All the primitives connecting the out-connection points of the target primitive are searched, and the searched primitives are stored in the TPIA in turn. The line between the target primitive and its connection primitive is stored in the TLIA.
(c) A primitive in the TPIA is removed in turn and marked as A_i, and the target primitive is updated toA_i; then loop step (b) is updated until all the primitives in the TPIA are traversed completely.

The abstract topology implementation flow chart is shown in Fig. 7.

In Fig. 7, p is the first-dimensional sequence number of the TPIA, q is the first-dimensional sequence number of the TLIA, and z is the first-dimensional sequence number of the target point in the TPIA. Because the first number of arrays in the computer is stored by default from 0, the initial values of p, q and z are set to 0.

k is the column number of the second-dimensional out-connection property in the PTIA. In the second-dimensional

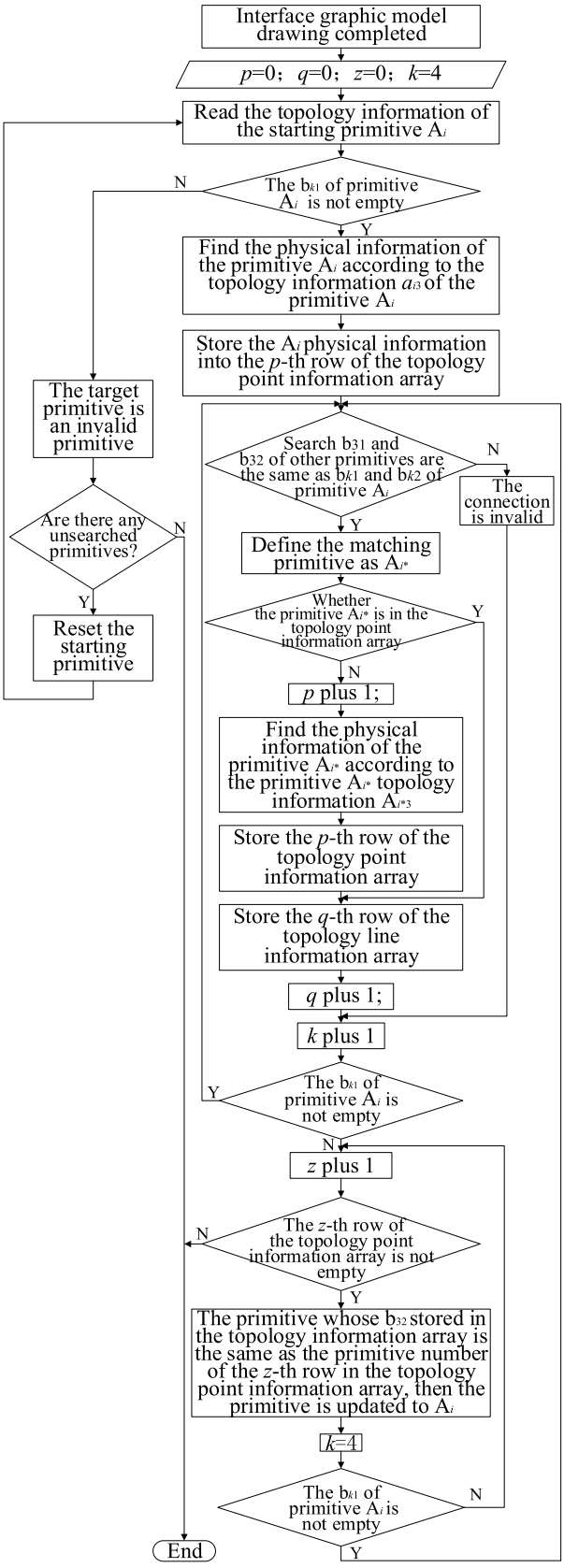

FIGURE 7. Flow chart of the abstract topology extraction.

TABLE 1. The third-dimensional numerical table of the topographical information array of primitives 1∼12.

Primitive number	Upper left corner coordinate	Lower right corner coordinates	Type and number of the primitive	Type and number of the out-connection primitive	Type and number of the out-connection primitive
1	$(b_{11},b_{12})_{a1}$	$(b_{21},b_{22})_{a1}$	$(b_{31},1)_{a1}$	$(b_{41},2)_{a1}$	$(b_{51},3)_{a1}$
2	$(b_{11},b_{12})_{a2}$	$(b_{21},b_{22})_{a2}$	$(b_{31},2)_{a2}$	$(\backslash,\backslash)_{a2}$	$(\backslash,\backslash)_{a2}$
3	$(b_{11},b_{12})_{a3}$	$(b_{21},b_{22})_{a3}$	$(b_{31},3)_{a3}$	$(b_{41},4)_{a3}$	$(b_{51},9)_{a3}$
4	$(b_{11},b_{12})_{a4}$	$(b_{21},b_{22})_{a4}$	$(b_{31},4)_{a4}$	$(b_{41},5)_{a4}$	$(b_{51},11)_{a4}$
5	$(b_{11},b_{12})_{a5}$	$(b_{21},b_{22})_{a5}$	$(b_{31},5)_{a5}$	$(b_{41},6)_{a5}$	$(b_{51},7)_{a5}$
6	$(b_{11},b_{12})_{a6}$	$(b_{21},b_{22})_{a6}$	$(b_{31},6)_{a6}$	$(\backslash,\backslash)_{a6}$	$(\backslash,\backslash)_{a6}$
7	$(b_{11},b_{12})_{a7}$	$(b_{21},b_{22})_{a7}$	$(b_{31},7)_{a7}$	$(b_{41},8)_{a7}$	$(\backslash,\backslash)_{a7}$
8	$(b_{11},b_{12})_{a8}$	$(b_{21},b_{22})_{a8}$	$(b_{31},8)_{a8}$	$(\backslash,\backslash)_{a8}$	$(\backslash,\backslash)_{a8}$
9	$(b_{11},b_{12})_{a9}$	$(b_{21},b_{22})_{a9}$	$(b_{31},9)_{a9}$	$(b_{41},10)_{a9}$	$(\backslash,\backslash)_{a9}$
10	$(b_{11},b_{12})_{a10}$	$(b_{21},b_{22})_{a10}$	$(b_{31},10)_{a10}$	$(\backslash,\backslash)_{a10}$	$(\backslash,\backslash)_{a10}$
11	$(b_{11},b_{12})_{a11}$	$(b_{21},b_{22})_{a11}$	$(b_{31},11)_{a11}$	$(b_{41},12)_{a11}$	$(\backslash,\backslash)_{a11}$
12	$(b_{11},b_{12})_{a12}$	$(b_{21},b_{22})_{a12}$	$(b_{31},12)_{a12}$	$(\backslash,\backslash)_{a12}$	$(\backslash,\backslash)_{a12}$

out-connection property, the front three columns are the upper left corner coordinates of the primitive, the lower right corner coordinates of the primitive, and the base property identification of the primitive. Therefore, the column number of the out-connection primitive property is from the 4th column, that is, k starts from 4.

B. MODEL TOPOLOGY RECOGNITION RESULTS

Through the above two mapping modes, the computer can complete the autonomous recognition of the HMIVSM and automatically interface the HMIVSM with the PSOSAA.

To further illustrate the effectiveness of the proposed method, the point-line topology diagram in Fig. 3 is taken as an example. The point-line topology identified using the proposed QSM method is shown in Fig. 8, and the corresponding abstract topology results and search order are also shown.

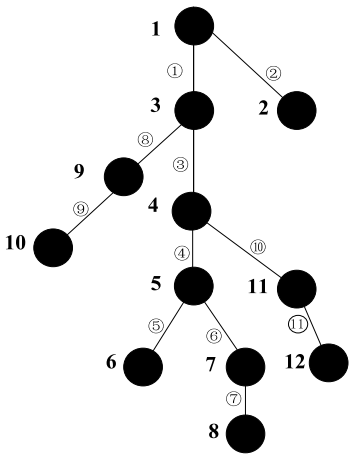

FIGURE 8. Point-line topology diagram after using QSM.

In Fig. 8, numbers 1-12 are point numbers, and numbers ①-⑪ are line numbers. After the primitive identification, the dimension of formula (3) is 12. The second dimension in the PTIA is set to 5, that is, $k = 5$ in formula (4).

The values of primitives 1-12 in the third dimension are shown in Table 1, where \ represents empty.

When the topology information of the primitive is searched in real time, the PTIA is completed simultaneously. Then the PPIA is completed according to the coordinate property of the primitive. After the mapping of the PIS is completed, ATS mapping is performed, and two two-dimensional arrays of the abstract topology are obtained; TPIA and TLIA. According to the point-line topology diagram shown in Fig. 8, the TPIA is shown in formula (10).

$$\begin{aligned} \boldsymbol{G} = \{&0(1,1,c_1),\ 1(2,2,c_2),\ 2(3,3,c_3),\ 3(4,4,c_4),\\ &4(5,9,c_9),\ 5(6,5,c_5),\ 6(7,11,c_{11}),\ 7(8,10,c_{10}),\\ &8(9,6,c_6),\ 9(10,7,c_7),\ 10(11,12,c_{12}),\ 11(12,8,c_8)\} \end{aligned} \tag{10}$$

where the integer set (0-11) is the first-dimensional serial number of the TPIA. The first integer set (1-12) in the second dimension is the sequence number of the searched points, and the second integer set (1-12) in the second dimension is the information number of the searched primitive. $c_1 - c_{12}$ in the second dimension correspond respectively to the physical information of the primitive marked using point (No.1-12) in Fig. 8.

The TLIA is shown in formula (11).

$$\begin{aligned} \boldsymbol{L} = \{&0(1,1,2,d_2),\ 1(2,1,3,d_1),\ 2(3,3,4,d_3),\ 3(4,3,5,d_8),\\ &4(5,4,6,d_4),\ 5(6,4,7,d_{10}),\ 6(7,5,8,d_9),\ 7(8,6,9,d_5),\\ &8(9,6,10,d_6),9(10,7,11,d_{11}),10(11,10,12,d_7)\} \end{aligned} \tag{11}$$

where the integer set (0-10) is the first dimension serial number of the TLIA. The first integer set (1-11) in the second dimension is sequentially arranged in order of the line search sequence number, and the second integer set and the third integer set in the second dimension are the first primitive point search sequence number of the searched line and the end primitive point search sequence number of the searched line, respectively. The primitive point search sequence numbers correspond to the first integer set of the second dimension in the TPIA that is G in formula (10). d_1 -d_{11} in the second dimension correspond to the physical information of

eleven lines. The serial numbers of eleven lines correspond to Nos. ①-⑪ in Fig. 8.

For example, the second dimension array (7, 5, 8, d_9) corresponding to the first dimension serial number is 6, and d_9 is is the physical information corresponding to line ⑨ in Fig. 8. The first number 7 is the search number of line ⑨ in Fig. 8, that is, the search order of line ⑨ is ranked seventh. The second number 5 is the first primitive point search sequence number of the line, and the primitive information number is 9 in Fig. 8. Formula (11) shows that the search sequence number of primitive information number 9 is 5. The third number 8 is the end primitive point search sequence number of the line, and the primitive information number is 10 in Fig. 8. Formula (11) shows that the search sequence number of the primitive information number 10 is 8.

In the process of forming the abstract topology, the TPIA and the TLIA are simultaneously performed. The point and line search sequence diagram is shown in Fig. 9. The red numbers 1-12 are the search sequence numbers of the abstract topology points, and the red numbers ①-⑪ are the search sequence numbers of the abstract topology lines.

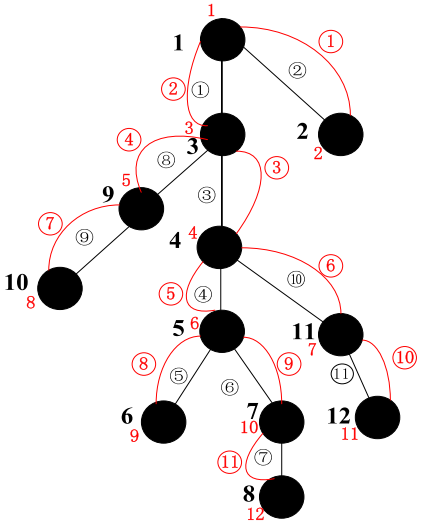

FIGURE 9. Point line search sequence diagram.

IV. DISTRIBUTION NETWORK SYSTEM MODELLING GRAPHIC TOPOLOGY AUTONOMIC IDENTIFICATION

A. IMGS

The MFC application framework based on Microsoft Visual Studio is used to develop an operation analysis simulation platform of the distribution network system [33]–[35]. The distribution network modelling system can be built on the human-machine interface of the platform. The physical properties of the primitives can be assigned. There are 11 kinds of primitives according to their function type: grid, bus, circuit breaker, switch, double winding transformer, three winding transformer, wire, inductor, capacitor, load, and ground. The HMIVSM of the distribution network system is shown in Fig. 10.

B. PIS

When the operator draws the HMIVSM on the working area of the human-computer interface, the boundary box of each primitive and its connection identification point have also been defined, that is, primitive recognition has been implemented.

First, the dimensions of the PTIA need to be set as follows.

(1) The first dimension of the PTIA is set to 100 according to the scale of the example distribution network system. That is, the dimension of formula (3) is 100.
(2) Since there may be multiple connections at the bus end, generally up to four, the dimension of the second dimension of the PTIA is set to 7. The dimension of formula (4) is 7, that is, $k = 7$.
(3) The dimension of the third dimension in the PTIA is set to 2.

Next, the dimensions of the PTIA need to be set as follows.

(1) The dimension of the first dimension in the PTIA is the same as the number of primitive function types; hence, it is set to 11. That is, the dimension of formula (7) is 11.
(2) The second dimension records the primitive number of each function type; hence, it is set to 100. That is, the dimension of formula (8) is 100.
(3) The third dimension records the number of physical properties of the primitive. Because the number of properties varies with type, the dimension must be set to the maximum value of all of them. The parameters of the three winding transformers have 6 properties whose number is maximum. Therefore, the dimension is set to 6. That is, the dimension of formula (9) is 6.

Finally, after the dimensions of the primitive information array are set as mentioned above, the visual graphic model of the distribution network system in the interface is converted into the primitive information array by the method of mapping mode 1 described in Section II.B.1. This conversion process is completed automatically by computer C/C++ language programming.

C. ATS

The conversion described in Section VI.B only completes the recognition of primitives in the HMIVSM of the distribution network system. However, the converted PIS cannot be directly interfaced with the programs of the distribution network analysis algorithms by the computer [36]–[40]. Therefore, mapping mode 2 in Section II.B.2 is used to convert the PIS into the ATS that can autonomously interface with the operation algorithm programs of the distribution network. The details are as follows:

The definition of points and lines in the point-line topology in this example refers to the definition of points and lines in the power system topology, that is, points in the power system topology are called nodes, and lines are called branches. For the specific needs of distribution network power flow analysis in the power system, the bus primitive is set as a node, and the branch is a combination of a logical connection and a

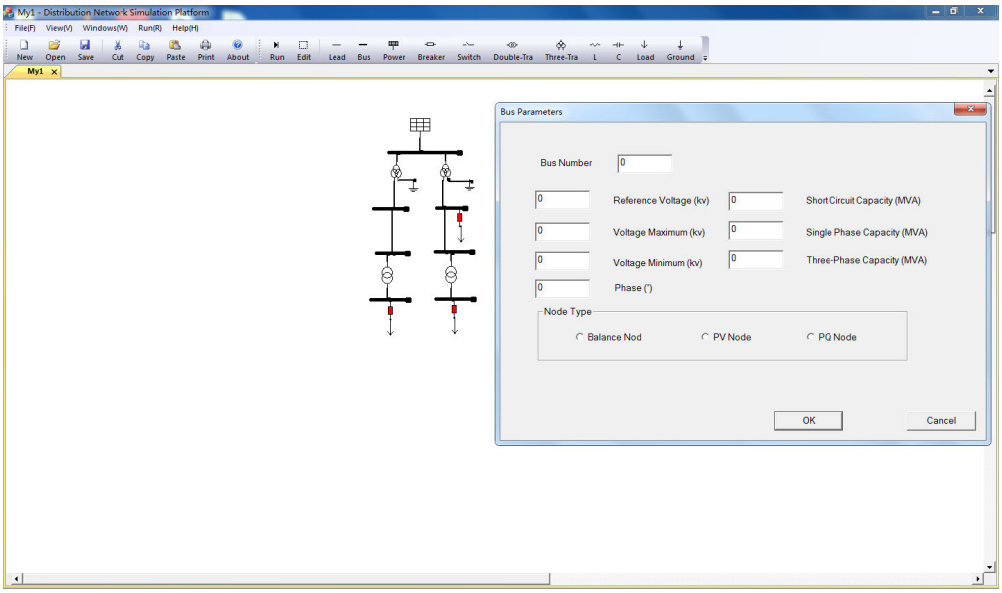

FIGURE 10. The interface graphic modelling diagram of the distribution network system.

physical connection; that is, a combination of the primitive other than the bus with its logical connection is regarded as a line. For example, the line connection between point 1 and point 2 in Fig. 11 is a combination of the logical connection of bus 1 and the three winding transformers, the three winding transformers, and the logical connection of the three winding transformers and bus 2. The point-line diagram obtained from the interface graphic model of the distribution network system in Fig. 10 is shown in Fig. 11.

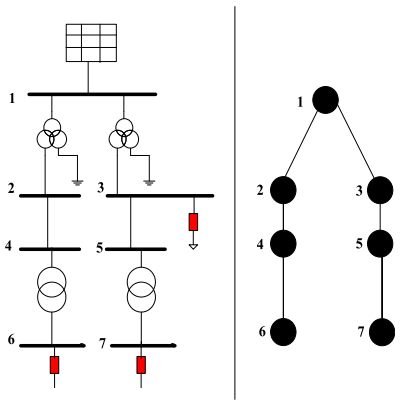

FIGURE 11. Point-line topology diagram of the distribution network system.

The TPIA and the TLIA are formed by using mapping mode 2 in Section II.B. There are special components such as circuit breakers and switches in the distribution network system, which will directly change the system topology. Therefore, it is necessary to specifically obtain information from the switch components to form a switch information array. When the topology change caused by this switch status changes, the TPIA and the TLIA are adjusted in time by the switch state change in the switch information array, and the switch information can be separately obtained to improve the speed of the node and branch information obtained. Furthermore, the conversion efficiency of the interface graphics topology is improved.

1) THE DIMENSION SETTING OF TPIA

The dimension of the first dimension of the TPIA in Section VI.B is set to 100. According to the physical information required for the distribution network power flow analysis, the dimension of the second dimension is set to 9. The stored information in the second dimension array includes the node search serial number, node information number, node type, reference voltage, node input active power, node input reactive power, node output active power, node output reactive power, and node susceptance.

2) THE DIMENSION SETTING OF TLIA

The dimension of the first dimension of the TLIA in Section VI.B is set to 100. The dimension of the second dimension is set to 5 according to the physical information required for the power flow analysis of the distribution network system. The storage information of the second dimension includes the search serial number of the branch, the search serial number of the branch input node, and the search serial number of the branch output node, branch resistance, and branch reactance.

3) THE DIMENSION SETTING OF THE SWITCH INFORMATION ARRAY

The first dimension represents the switch number, and its dimension is set to 100. The dimension of the second dimension is set to 4 according to the physical information of the switch. The storage information of the second dimension includes the information number of the switch, the on/off

TABLE 2. Bus parameters.

Bus number	Voltage (kV)	Node type
1	220	Balanced node
2	110	PQ node
3	110	PQ node
4	110	PQ node
5	110	PQ node
6	10	PQ node
7	10	PQ node

TABLE 3. Wire parameters.

Wire number	Unit resistance (Ω/km)	Unit reactance (Ω/km)	Unit susceptance (S/km)	Length (km)
L_1	0.063	0.270	4.4922×10^{-6}	7.9
L_2	0.063	0.270	4.4922×10^{-6}	7.9

state of the switch, the search serial number of the switch input node, and the search serial number of the switch output node.

The physical parameters of each primitive in the distribution network model are assigned through the interface dialog as shown in Fig. 10, and each primitive in the model is consistent with the number shown in FIG. 11.

The bus parameters are shown in Table 2.

The wire parameters are shown in Table 3.

The transformer parameters are shown in Table 4.

The power loss of load M_1 is (15+j2.1)MVA, the power loss of load M_2 is (20+j2.9)MVA.

The conversion process is automatically completed by computer C\C++ language programming. The node information array and the branch information array in abstract topology space converted from the interface modelling space are output to the TXT file. The results are shown in Fig. 12 and Fig. 13, which verify the feasibility and correctness of the proposed QSM method.

D. THE AUTOMATIC INTERFACE IMPLEMENTATION WITH SYSTEM OPERATION SIMULATION ALGORITHM

Using the proposed method, the HMIVSM in Fig. 10 is autonomously identified and converted into an abstract topology information array shown in Fig. 12 and Fig. 13 in Section VI.C.

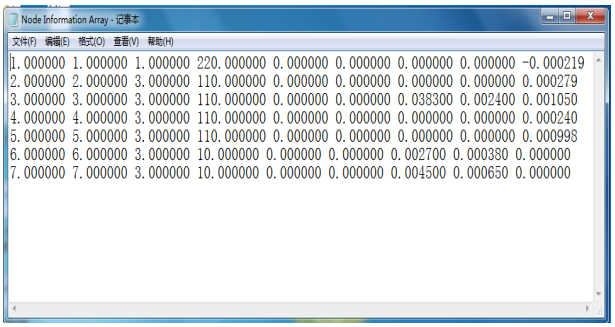

FIGURE 12. Node information array.

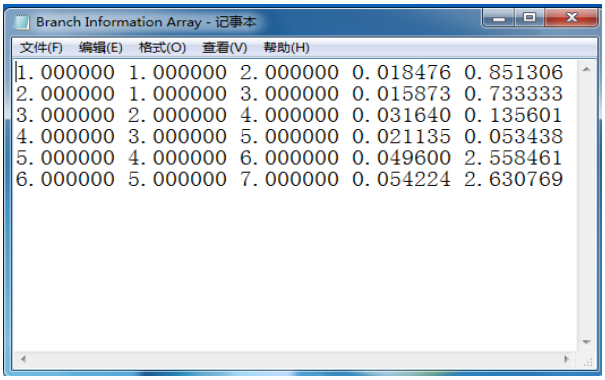

FIGURE 13. Branch information array.

To further verify the effectiveness of the proposed method in realizing the operation simulation analysis of the system visualization model and verify the correctness of the automatic interface, the converted abstract topology is verified with the programs of the system operation algorithm. The C/C++ language is used to program the forward push-back iteration power flow calculation method of the distribution network system [41]–[43]. The converted abstract topology information arrays can be directly read as the input data of the power flow calculation algorithm.

The results of the system power flow calculation simulation are shown in Fig. 14. It is shown that the proposed QSM method is effective and feasible for converting the visual interface model into an abstract topology that can be autonomously interfaced with the programs of the system operation simulation algorithm. It has a certain effect on the realization of the human-machine interface visualization system operation analysis platform and plays a key role in promoting computer development in terms of human-machine interface graphic self-identification technology.

TABLE 4. Transformer parameters.

Transformer number	Voltage (kV)	Standard capacity (MVA)	Standard capacity ratio	Short circuit loss (kW)	Short circuit voltage (%)	No-load current (%)
T_1, T_2	220\121\10.5	180	2:2:1	514.3\203.4\148.6	13.2\23.5\7.72	0.065
T_3, T_4	110\10.5	50	1:1	176.227	17.1	0.081

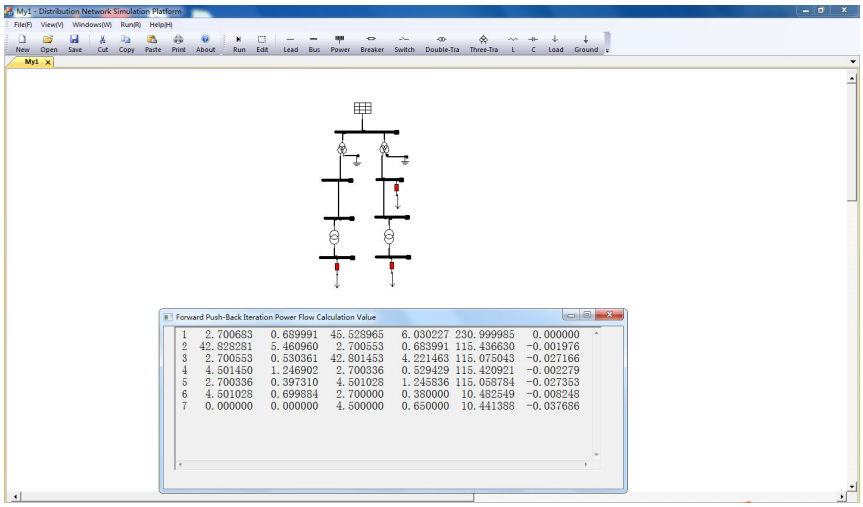

FIGURE 14. The results of forward push-back iteration power flow calculation.

V. CONCLUSION

This paper studies an autonomous identification method of human-machine interface modelling graphics topology. The definition of QSM is formulated, and a mathematical model is derived. The paper also explains in detail three topological spaces, two mapping methods and their implementation methods in the automatic identification process of an HMIVSM and its conversion into an abstract topology by a computer. Combining machine language programming, the proposed QSM method can perfectly interface the HMIVSM with the PSOSAA. The QSM method is more intuitive and convenient for the visualization and operational analysis of the system. Finally, taking the distribution network system as an example, the effectiveness and correctness of the proposed QSM method are verified for the automatic identification of the HMIVSM by a computer. Its effectiveness and correctness are also verified by an autonomous interface with the programs of the power flow algorithms.

The proposed algorithm in this paper provides a certain reference point in the computerized autonomic identification of interface modelling graphics topology, and it has certain universality. The proposed algorithm can be extended to complex systems that need to develop graphical modelling using a computer visualization interface, identify the HMIVSM by the computer itself, and then interface with the programs of the system operation algorithms to analyse system operation. Further research will focus on the optimization of topology identification procedures and the efficiency of data processing when the system has great scale and the data are large.

REFERENCES

[1] S. M. Mirić and P. V. Pejović, "A method for computer-aided analysis of differential mode input filters," *IEEE Trans. Ind. Electron.*, vol. 64, no. 6, pp. 4741–4750, Jun. 2017.

[2] S. Habibkhah, J. Arasi, and H. Bolandi, "SPACSSIM: Simulation and analysis software for mathematical modeling of satellite position and attitude control systems," *Comput. Sci. Eng.*, vol. 19, no. 5, pp. 38–48, 2017.

[3] J. Ossorio, J. Vague, V. E. Boria, and M. Guglielmi, "Exploring the tuning range of channel filters for satellite applications using electromagnetic-based computer aided design tools," *IEEE Trans. Microw. Theory Techn.*, vol. 66, no. 2, pp. 717–725, Feb. 2018.

[4] D. I. Katzourakis, N. Lazic, C. Olsson, and M. R. Lidberg, "Driver steering override for lane-keeping aid using computer-aided engineering," *IEEE/ASME Trans. Mechatronics*, vol. 20, no. 4, pp. 1543–1552, Aug. 2015.

[5] T. D. Chellan and A. K. Chellappan, "Novel computer-aided diagnosis of lung cancer using bag of visual words to achieve high accuracy rates," *J. Eng.*, vol. 2018, no. 12, pp. 1941–1946, Dec. 2018.

[6] L. Sallemi, I. Njeh, and S. Lehericy, "Towards a computer aided prognosis for brain glioblastomas tumor growth estimation," *IEEE Trans. Nanobiosci.*, vol. 14, no. 7, pp. 727–733, Oct. 2015.

[7] Z. Tian, W. Wu, and B. Zhang, "A mixed integer quadratic programming model for topology identification in distribution network," *IEEE Trans. Power Syst.*, vol. 31, no. 1, pp. 823–824, Jan. 2016.

[8] M. Babakmehr, M. G. Simões, M. B. Wakin, and F. Harirchi, "Compressive sensing-based topology identification for smart grids," *IEEE Trans. Ind. Informat.*, vol. 12, no. 2, pp. 523–543, Apr. 2016.

[9] S. Pan, Y. Zhou, F. Yu, F. Qian, and G. Hu, "Network topology tomography under multipath routing," *IEEE Commun. Lett.*, vol. 20, no. 3, pp. 550–553, Mar. 2016.

[10] M. Babakmehr, M. G. Simoes, M. B. Wakin, A. A. Durra, and F. Harirchi, "Smart-grid topology identification using sparse recovery," *IEEE Trans. Ind. Appl.*, vol. 52, no. 5, pp. 4375–4384, Sep. 2016.

[11] G. Cavraro and V. Kekatos, "Graph algorithms for topology identification using power grid probing," *IEEE Control Syst. Lett.*, vol. 2, no. 4, pp. 689–694, Oct. 2018.

[12] Y. Weng, Y. Liao, and R. Rajagopal, "Distributed energy resources topology identification via graphical modeling," *IEEE Trans. Power Syst.*, vol. 32, no. 4, pp. 2682–2693, Jul. 2017.

[13] A. Sagrista, S. Jordan, A. Just, F. Dias, L. G. Nonato, and F. Sadlo, "Topological analysis of inertial dynamics," *IEEE Trans. Vis. Comput. Graphics*, vol. 23, no. 1, pp. 950–959, Jan. 2017.

[14] B. Rieck, U. Fugacci, J. Lukasczyk, and H. Leitte, "Clique community persistence: A topological visual analysis approach for complex networks," *IEEE Trans. Vis. Comput. Graphics*, vol. 24, no. 1, pp. 822–831, Jan. 2018.

[15] J. Xia, F. Ye, F. Zhou, Y. Chen, and X. Kui, "Visual identification and extraction of intrinsic axes in high-dimensional data," *IEEE Access*, vol. 7, pp. 79565–79578, 2019.

[16] C. Mao, F. Leng, J. Li, S. Zhang, L. Zhang, R. Mo, D. Wang, J. Zeng, X. Chen, R. An, and Y. Zhao, "A 400-V/50-kVA digital–physical hybrid real-time simulation platform for power systems," *IEEE Trans. Ind. Electron.*, vol. 65, no. 5, pp. 3666–3676, May 2018.

[17] M. D. O. Faruque, T. Strasser, G. Lauss, V. Jalili-Marandi, P. Forsyth, C. Dufour, V. Dinavahi, A. Monti, P. Kotsampopoulos, J. A. Martinez, K. Strunz, M. Saeedifard, X. Wang, D. Shearer, and M. Paolone, "Real-time simulation technologies for power systems design, testing, and analysis," *IEEE Power Energy Technol. Syst. J.*, vol. 2, no. 2, pp. 63–73, Jun. 2015.
[18] I. Mahmood, T. Kausar, H. S. Sarjoughian, A. W. Malik, and N. Riaz, "An integrated modeling, simulation and analysis framework for engineering complex systems," *IEEE Access*, vol. 7, pp. 67497–675148, 2019.
[19] C. Shum, W.-H. Lau, T. Mao, H. S.-H. Chung, K.-F. Tsang, N. C.-F. Tse, and L. L. Lai, "Co-simulation of distributed smart grid software using direct-execution simulation," *IEEE Access*, vol. 6, pp. 20531–20544, 2018.
[20] L. Xu, T. W. S. Chow, and E. W. M. Ma, "Topology-based clustering using polar self-organizing map," *IEEE Trans. Neural Netw. Learn. Syst.*, vol. 26, no. 4, pp. 798–808, Apr. 2015.
[21] K. Tasdemir, P. Milenov, and B. Tapsall, "Topology-based hierarchical clustering of self-organizing maps," *IEEE Trans. Neural Netw.*, vol. 22, no. 3, pp. 474–485, Mar. 2011.
[22] J. Li and M. Chen, "Multiobjective topology optimization based on mapping matrix and NSGA-II for switched industrial Internet of Things," *IEEE Internet Things J.*, vol. 3, no. 6, pp. 1235–1245, Dec. 2016.
[23] Q. Zheng, J. Li, H. Tian, Z. Wang, and S. Wang, "A 2-layers virtual network mapping algorithm based on node attribute and network simplex," *IEEE Access*, vol. 6, pp. 77474–77484, 2018.
[24] W. Liang, H. Liangang, and X. Xihai, "Research on the implementation of topology mapping algorithm in intelligent cloud test," *Comput. Technol. Appl.*, vol. 43, no. 3, pp. 116–119, 2017, doi: 10.16157/j.issn.0258-7998.2017.03.029.,
[25] L. Yuan, Q. Changling, W. Xiaofeng, and J. Min, "Research on topology mapping method for multiscale integration network emulation," *J. Syst. Simul.*, vol. 31, no. 10, p. 2030, Oct. 2019.
[26] J. Hey, T. J. Teo, V. P. Bui, G. Yang, and R. Martinez-Botas, "Electromagnetic actuator design analysis using a two-stage optimization method with coarse–fine model output space mapping," *IEEE Trans. Ind. Electron.*, vol. 61, no. 10, pp. 5453–5464, Oct. 2014.
[27] W. Yanjuan, W. Haoyue, and Y. Li, "Research on modeling method of visualized plane topology in electric power system," in *Proc. 38th Chin. Control Conf. (CCC)*, Jul. 2019, pp. 7263–7268.
[28] T. Zheng, *Space Mapping*. Beijing, China: Science Press, 2014, ch. 4, pp. 60–64.
[29] H. Liu, Y. Tian, H. Zong, Q. Ma, M. Y. Wang, and L. Zhang, "Fully parallel level set method for large-scale structural topology optimization," *Comput. Struct.*, vol. 221, pp. 13–27, Sep. 2019, doi: 10.1016/j.compstruc.2019.05.010.
[30] C.-W. Ten, E. Wuergler, H.-J. Diehl, and H. B. Gooi, "Extraction of geospatial topology and graphics for distribution automation framework," *IEEE Trans. Power Syst.*, vol. 23, no. 4, pp. 1776–1782, Nov. 2008.
[31] J. Yu, Y. Weng, and R. Rajagopal, "PaToPaEM: A data-driven parameter and topology joint estimation framework for time-varying system in distribution grids," *IEEE Trans. Power Syst.*, vol. 34, no. 3, pp. 1682–1692, May 2019.
[32] C. Chaoqun and Q. Ping, "Topology identification and simulation based on multi-agent system in microgrid," *Mod. Electron. Techn.*, vol. 39, no. 11, pp. 149–151, Mar. 2018, doi: 10.16652/j.issn.1004-373X.2016.11.036.
[33] W. Kai, *Implementation and Application of Power System Graphic Modeling Simulation Software System*. Hefei, China: Anhui Univ., 2013, pp. 11–26.
[34] J. Prosise, *Programming Windows With MFC*, 2nd ed. Beijing, China: Tsinghua Univ. Press, 2001, pp. 24–57.
[35] D. Hearn, M. P. Baker, and W. R. Carithers, *Computer Graphics With OpenGL*, S. J. Cai and R. Y. Yang, Eds., 4th ed. Beijing, China: Publishing House of Electronics Industry, 2014, pp. 5–23.
[36] A. T. Runkler and C. J. Bezdek, "Topology preserving feature extraction with multiswarm optimization," in *Proc. IEEE Int. Conf. Syst., Man, Cybern.*, Oct. 2013, pp. 2997–3002, doi: 10.1109/SMC.2013.511.
[37] R. Aoun, C. E. Abosi, E. A. Doumith, R. Nejabati, M. Gagnaire, and D. Simeonidou, "Towards an optimized abstracted topology design in cloud environment," *Future Gener. Comput. Syst.*, vol. 29, no. 1, pp. 46–60, Jan. 2013, doi: 10.1016/j.future.2012.03.024.
[38] M. Sedaghat, F. Hernández-Rodriguez, and E. Elmroth, "Decentralized cloud datacenter reconsolidation through emergent and topology-aware behavior," *Future Gener. Comput. Syst.*, vol. 56, pp. 51–63, Mar. 2016, doi: 10.1016/j.future.2015.09.023.
[39] L. Eskandari, J. Mair, Z. Huang, and D. Eyers, "T3-scheduler: A topology and traffic aware two-level scheduler for stream processing systems in a heterogeneous cluster," *Future Gener. Comput. Syst.*, vol. 89, pp. 617–632, Dec. 2018, doi: 10.1016/j.future.2018.07.011.
[40] W. Bai, J. Ren, and T. Li, "Modified genetic optimization-based locally weighted learning identification modeling of ship maneuvering with full scale trial," *Future Gener. Comput. Syst.*, vol. 93, pp. 1036–1045, Apr. 2019, doi: 10.1016/j.future.2018.04.021.
[41] L. Huijia, L. Ben, L. Xiaobing, and L. Jun, "Fast forward-pushing back-generation algorithm for distribution network with distributed power supply," *Water Resour. Power*, vol. 34, no. 6, pp. 213–216, Jun. 2016.
[42] F. Huo, P. Wang, X. Gong, D. Jiao, and Q. Ge, "Evaluation method of PV array of running status based on layered and divisional forward and backward algorithm," *Power Syst. Protection Control*, vol. 44, no. 15, pp. 68–72, Jul. 2016.
[43] C. Heng, *Power System Steady State Analysis*, 3rd ed. Beijing, China: China Electric Power Press, 2013, ch. 4, pp. 99–104.

YANJUAN WU received the M.S. and Ph.D. degrees in power systems and automation from Tianjin University, Tianjin, China, in 2005 and 2013, respectively. She is currently an Associate Professor with the School of Electrical and Electronic Engineering, Tianjin University of Technology. Her current research interests include intelligent control, smart grids, and grid optimization and control.

HAOYUE WANG was born in Handan, Hebei, China. She is currently pursuing the degree with the School of Electrical and Electronic Engineering, Tianjin University of Technology. She joined the School of Electrical and Electronic Engineering, in 2017. Her major is electrical engineering. Her main research interest includes smart grids. Her research interests include the development of power system modelling platform and algorithm research.

YUNLIANG WANG received the M.S. degree in power systems and automation from Tianjin University, Tianjin, China, in 1988. He is currently a Professor with the School of Electrical and Electronic Engineering, Tianjin University of Technology. His current research interests include intelligent control, multimotor coordinated control, microcomputer control, and power electronics technology.

LI YANG received the master's degree in power systems and automation from Tianjin University, in 2005. He is currently the Deputy Senior Electrical Engineer. His research interests include smart grids, grid regulation, and grid optimization and control.